DETERMINATION OF LIMITING HOLE-FLANGING COEFFICIENT IN AA1050-O ALUMINUM ALLOY SHEETS USING THE COCKROFT-LATHAM DUCTILE FRACTURE CRITERION

XÁC ĐỊNH HỆ SỐ NONG LỖ GIỚI HẠN CỦA TẤM HỢP KIM NHÔM AA1050-O SỬ DỤNG TIÊU CHUẨN PHÁ HỦY DẺO COCKROFT-LATHAM

Tran Duc Hoan[1,*], To Thanh Loan[2], Ta Duc Canh[3]

DOI: http://doi.org/10.57001/huih5804.2024.375

ABSTRACT

Hole-flanging is a crucial operation in sheet metal forming technology, where the material around a pre-fabricated hole is deformed by a spherical, conical, or cylindrical punch to create a flanged hole wall. This study aims to determine the limiting hole-flanging coefficient of AA1050-O aluminum alloy sheet using the Cockroft-Latham ductile fracture criterion. Numerical simulations of the hole-flanging process using the Cockroft-Latham ductile fracture criterion were conducted to identify the limiting hole-flanging coefficient of AA1050-O aluminum alloy sheet. The limiting hole-flanging coefficient of the material was found to be 0.61 and was further verified through experiments. Additionally, the effects of the hole-flanging coefficient on the Cockroft-Latham damage value, minimum thickness, and height of the flanged hole wall were evaluated within the formability region of the material when the coefficient exceeded the limiting value. The findings from this study provide valuable insights for designing hole-flanging operations for AA1050-O aluminum alloy sheet.

Keywords: *Hole-flanging, ductile fracture criterion, damage, simulation, experiment.*

TÓM TẮT

Nong lỗ là nguyên công quan trọng được sử dụng rộng rãi trong công nghệ tạo hình kim loại tấm, trong đó vật liệu xung quanh một lỗ được chế tạo trước bị biến dạng bởi chày có dạng cầu, côn hoặc trụ để tạo nên thành lỗ nong. Nghiên cứu này nhằm xác định hệ số nong lỗ giới hạn của tấm hợp kim nhôm AA1050-O sử dụng tiêu chuẩn phá hủy dẻo Cockroft-Latham. Các mô phỏng số quá trình nong lỗ sử dụng tiêu chuẩn phá hủy dẻo Cockroft-Latham được thực hiện để xác định hệ số nong lỗ giới hạn của tấm hợp kim nhôm AA1050-O. Hệ số nong lỗ giới hạn của vật liệu tìm được là 0.61, được phân tích và xác minh thêm thông qua các thực nghiệm. Ngoài ra, các ảnh hưởng của hệ số nong lỗ đến giá trị thiệt hại Cockroft-Latham, chiều dày tối thiểu và chiều cao của thành lỗ nong đã được đánh giá trong vùng khả năng tạo hình của vật liệu khi hệ số nong lớn hơn giá trị giới hạn. Những phát hiện từ nghiên cứu này cung cấp những hiểu biết có giá trị cho việc thiết kế các nguyên công nong lỗ đối với các tấm hợp kim nhôm AA1050-O.

Từ khóa: *Nong lỗ, tiêu chuẩn phá hủy dẻo, thiệt hại, mô phỏng, thực nghiệm.*

[1]Faculty of Mechanical Engineering, Le Quy Don Technical University, Vietnam
[2]School of Materials Science and Engineering, Hanoi University of Science and Technology, Vietnam
[3]183 Mechanical one member limited liability company (Z183 Factory), Vietnam
[*]Email: tranduchoan@lqdtu.edu.vn
Received: 21/8/2024
Revised: 15/11/2024
Accepted: 28/11/2024

1. INTRODUCTION

Hole-flanging is a manufacturing process that involves bending and stretching metal around a pre-fabricated hole by pressing a conical, spherical, or cylindrical punch through a die. Initially, a hole is created by drilling or punching, after which the metal

surrounding the hole is expanded to form a flanged hole wall. Throughout this process, the metal portion of the blank in contact with the die surface remains largely undeformed, as illustrated in Figure 1. The clearance between the punch and die can be either narrow or wide, depending on the desired shape of the flanged hole wall. Stretching the metal around the initial hole subjects the material to significant tangential tensile stress, resulting in substantial tangential tensile strain. This phenomenon can lead to thinning, necking, and even failure at the edge of the flanged hole wall. As the ratio of the initial hole diameter to the flanged hole diameter decreases, the tangential tensile strain at the flanged hole edge increases [1, 2]. This ratio, which characterizes the degree of material deformation during the hole-flanging process, is referred to as the hole-flanging coefficient (m_{HF}), while its inverse value is known as the hole-flanging ratio (K_{HF}) [3-5]:

$$m_{HF} = \frac{d_0}{d_p}; K_{HF} = \frac{1}{m_{HF}} = \frac{d_p}{d_0} \quad (1)$$

where d_0 is the diameter of the initial hole (in mm), and d_p is the punch diameter or the inner diameter of the flanged hole (in mm), as shown in Figure 1.

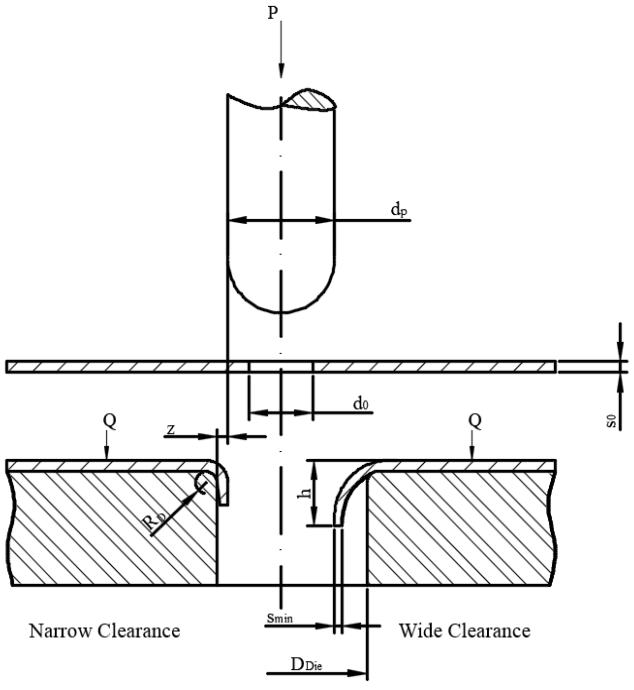

Figure 1. Schematic of the hole-flanging process

The part formed after the Hole-flanging process possesses a flanged hole wall with a height of h and a minimum thickness at the edge of the flanged hole wall, denoted as s_{min}, as illustrated in Figure 1. The material's ability to undergo hole-flanging is defined by the limiting hole-flanging coefficient. If the process is carried out with a coefficient below this limiting value, material failure will occur.

V. Kumar et al. conducted a study that combined both numerical simulation and experimental approaches to investigate the hole-flanging ability of 1.6mm thick AA6061-O aluminum alloy sheets, using the Swift and Voce strain hardening models [2]. The results demonstrated that, although both models predicted the maximum thinning at the edge of the flanged hole in good agreement with experimental observations, the limiting hole-flanging ratio predicted by the Swift strain hardening model exhibited better agreement with experimental data compared to the Voce strain hardening model.

F. Stachowicz experimentally determined the hole-flanging ability of DQ, DDQ, and EDQ steel sheets with a thickness of 1.0mm using three types of punches: conical, hemispherical, and cylindrical. The initial holes were prepared by drilling and punching [4]. The results revealed that the limiting hole-flanging ratio is influenced by the punch shape, the method of hole preparation, the material's anisotropy, and its strain hardening exponent. Thus, the yield and fracture behavior of the material are critical factors in predicting its hole-flanging ability. This finding is consistent with results reported by V. Kumar et al. [2], D.I. Hyun et al. [6], M. Borrego et al. [7], S. E. Seyyedi et al. [8].

M. Borrego et al. analyzed the formability of AA7075-O aluminum alloy sheets during the hole-flanging process using Single-Point Incremental Forming (SPIF), evaluated through the limiting hole-flanging ratio and the Forming Limit Curve (FLC) [7]. The study involved hole-flanging experiments with three cylindrical punches of varying fillet radii and one hemispherical punch, supplemented by numerical simulations of the deformation process. The results indicated that the limiting hole-flanging ratio is an effective measure of formability during hole-flanging by SPIF and is independent of the punch's fillet radius. In contrast, the conventional FLC was found to be unsuitable for analyzing the material's formability along the flanged hole wall, except at the edge of the flanged hole. Furthermore, the study revealed that the ductile fracture behavior, as analyzed using the FLC, was inadequate. The non-proportionality of strain paths during deformation and the local bending induced by the punch's fillet radius

were identified as critical factors explaining why successfully formed flanges exceeded the FLC without failure.

S. E. Seyyedi et al. employed the Modified Mohr-Coulomb (MMC) ductile fracture criterion, as proposed by Bai and Wierzbicki [9], to assess the formability of AA6061-T6 aluminum alloy sheets in both conventional hole-flanging (CHF) and incremental hole-flanging (IHF) [8]. The results demonstrated that the ductile fracture criterion accurately provides predictions for both processes. Additionally, it was found that the limiting formability in CHF was greater than that in single-stage IHF. However, the MMC ductile fracture criterion [9] depends on dimensionless stress variables, such as stress triaxiality and the normalized Lode angle parameter, as well as three material constants and coefficients from the strain-hardening model. Consequently, identifying these material constants can be challenging and prone to errors due to data processing and experimental system limitations.

Recently, ductile fracture criteria have been extensively utilized to assess the formability of metals [10-14]. The critical damage value of AA1050-O aluminum alloy sheets, determined using the Freudenthal, Cockroft-Latham, and normalized Cockroft-Latham ductile fracture criteria, was used to predict failure in the combined drawing process [10]. The findings demonstrated the superiority of the Cockroft-Latham criterion over other criteria in predicting both failure and non-failure occurrences in the combined deep drawing processes. Moreover, the Cockroft-Latham criterion showed greater accuracy in predicting failure positions in the Erichsen cupping test. The Cockroft-Latham damage critical value (C_{CL}) was determined using the formula [15]:

$$C_{CL} = \int_0^{\bar{\varepsilon}_f} \sigma_1 d\bar{\varepsilon} \quad (2)$$

where, σ_1 - the maximum principal stress, MPa; $\bar{\varepsilon}_f$ - the equivalent strain when the fracture occurred; $\bar{\varepsilon}$ - the equivalent strain; C_{CL} - critical damage values known as material constants, MJ/m^3. According to the Cockroft-Latham ductile fracture criterion, the damage value is based on the maximum principal stress and the equivalent strain, making it particularly suitable for predicting hole-flanging ability. This is because, during the hole-flanging process, the tangential tensile stress reaches its peak value at the edge of the flanged hole, which is the primary cause of damage. However, to date, no comprehensive study has investigated the limiting hole-flanging ability using the Cockroft-Latham criterion.

This paper presents a study aimed at determining the hole-flanging ability of AA1050-O aluminum alloy sheets with a thickness of 2.0mm through the limiting hole-flanging coefficient. Numerical simulations of the hole-flanging process, utilizing the Cockroft-Latham ductile fracture criterion, were performed to establish the value of the limiting hole-flanging coefficient. Experiments of the hole-flanging process were conducted according to the simulations to evaluate the accuracy of the predicted results. Additionally, the dependence of the Cockroft-Latham damage value, the minimum thickness, and the height of the flanged hole wall on the hole-flanging coefficient was identified. The findings provide valuable insights for engineers in designing the technological process of the hole-flanging operation.

2. MATERIAL AND METHODOLOGY

Numerical simulations of the hole-flanging process were conducted based on the finite element method implemented in Deform 2D software using the Cockroft-Latham ductile fracture criterion for an AA1050-O aluminum alloy blank with a thickness of 2.0mm, an outer diameter of 92mm, and variable initial hole diameters of 12mm, 13mm, 14mm, 15mm, and 16mm, as shown in Figure 2. The geometric model used in the simulations was axisymmetric, consisting of a hemispherical punch with a diameter of 20mm, a die with an inner diameter of 27mm, a die edge fillet radius of 0.75mm, and an outer diameter of 55mm. The blank holder had an inner diameter of 33 mm and an outer diameter of 55mm. The punch movement speed was set to 4.0mm/s, and the blank holder force was 10,000N. The simulation consisted of 501 steps, with each step moving the punch by 0.05mm. The clearance between the punch and die was 3.5mm, which exceeded the blank thickness of 2.0mm. The coefficient of friction between the blank and the tool was set at 0.12, using VBC Fine Punch-150N lubricant.

The flow curve of blank material was described using the Swift model $\sigma = K(\varepsilon_0 + \varepsilon)^n$, where σ is the true stress (MPa), ε is the true strain, K is the strength coefficient (K = 132MPa), ε_0 is the pre-strain ($\varepsilon_0 = 0.0005$), and n is the strain hardening exponent (n = 0.285) [16]. The elastic property of the material was determined by a Young's modulus of 69GPa and a Poisson's ratio of 0.33 [17]. The workpiece was meshed with 2D elements in equal squares, each with dimensions of 0.1mm x 0.1mm.

A Cockroft-Latham critical damage value of 61.49MJ/m^3, as determined from the reported study [10], was used. Through numerous numerical simulations, the minimum initial hole diameter d_0 required to ensure that the product remains undamaged was identified. The failure condition of the material was assessed using the Cockroft-Latham ductile fracture criterion.

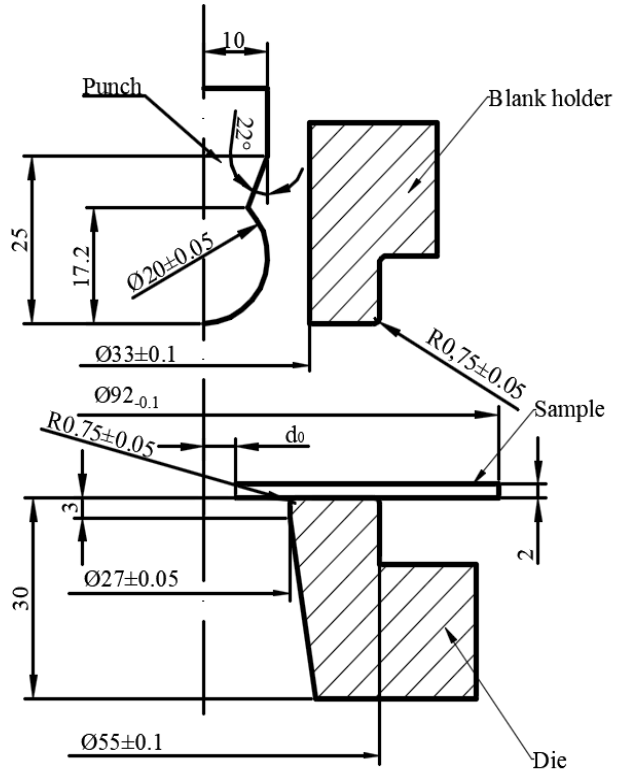

Figure 2. Numerical simulation model for the hole-flanging process

The experiments corresponding to the numerical simulations were conducted using an Erichsen Model 111 at the Metal Forming Laboratory of Le Quy Don Technical University. The experimental toolset and the AA1050-O aluminum alloy blanks were prepared with the same dimensions as those used in the simulation model. The holes in the blanks were created by drilling. The analysis of both experimental and simulation results facilitated the evaluation of the hole-flanging ability of the material and the effectiveness of the Cockroft-Latham criterion. Additionally, the influence of the hole-flanging coefficient on the Cockroft-Latham damage value, minimum thickness, and height of the flanged hole wall was also assessed Surface observations of the openings of the flanged hole walls after the hole-flanging process were conducted using a ZEISS Axio Imager A2m microscope at the Materials Laboratory of Le Quy Don Technical University. The captured images were used to evaluate crack formation.

3. RESULTS AND DISCUSSION

3.1. Simulation results

The simulation results are shown in Figure 3. The color scale represents the Cockroft-Latham damage values, corresponding to the color distribution on the formed part. A higher Cockroft-Latham damage value indicates an increased risk of material failure. The material fails at the position where this value reaches the critical value, C_{CL} = 61.49MJ/m^3. In the simulations, the highest Cockroft-Latham damage value was identified at the edge of the flanged hole wall, where the tensile stress and tensile strain in the tangential direction are greatest. The elements at the edge of the flanged hole wall of the initial blank with diameter d_0 were stretched to match the diameter of the 20mm punch.

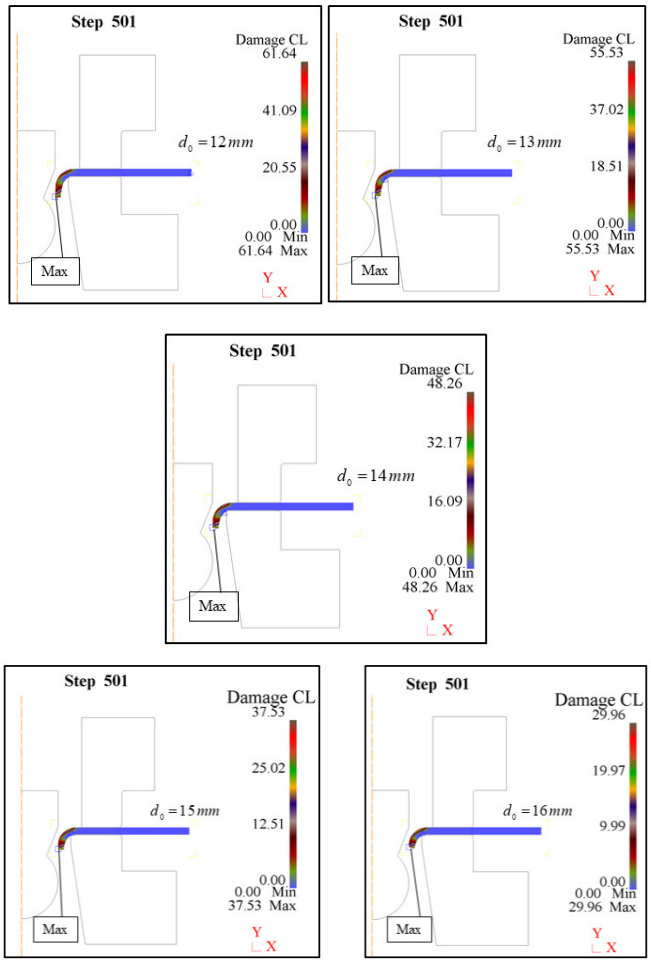

Figure 3. Cocroft-Latham damage value

It can be observed that as the hole diameter decreases, the damage value increases, corresponding to a reduction in the hole-flanging coefficient. When the initial hole diameter is 12mm, the maximum Cockroft-Latham damage value reaches 61.64MJ/m^3, exceeding

the critical damage value C_{CL}. This indicates that failure has occurred at the edge of the flanged hole wall, specifically at the inner edge where it contacts the punch. This result is consistent with the expected outcomes of the hole-flanging process and aligns with previously published findings [2, 4-8]. For hole diameters of 13mm, 14mm, 15mm, and 16mm, no failure was predicted by the Cockroft-Latham criterion.

Figure 4 illustrates the relationship between the maximum Cockroft-Latham damage value and the hole-flanging coefficient. The maximum Cockroft-Latham damage value was approximated by a first-order function. The intersection of this function with the Cockroft-Latham critical damage curve (C_{CL} = 61.49) was used to determine the limiting hole-flanging coefficient. The expression for the maximum Cockroft-Latham damage value is given by the following formula:

$$C_{CL}^{max} = 160.488 - 162.72 m_{HF} \quad (3)$$

where m_{HF} is the hole-flanging coefficient.

As the hole-flanging coefficient increases, the maximum Cockroft-Latham damage value decreases. The results demonstrated that the limiting hole-flanging coefficient for the AA1050-O aluminum alloy sheet was determined to be 0.61, corresponding to an initial hole diameter of 12.2mm.

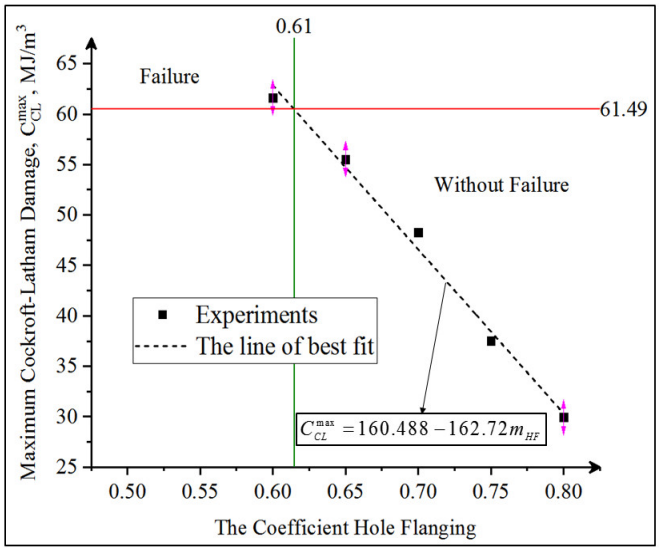

Figure 4. Dependence of the maximum Cockroft-Latham damage value on the hole-flanging coefficient

The simulation results also illustrate the distribution of material thickness and the height of the flanged hole, specifically for an initial hole diameter of 12mm, as shown in Figure 5. The initial blank thickness gradually decreases from the radius of the die edge to the edge of the flanged hole wall. The minimum thickness occurs at the edge of the flanged hole wall, where, for an initial hole diameter of 12mm, the minimum thickness was identified to be 1.37mm. The material thickness distribution of the part after the hole-flanging process is consistent with previously published results [18, 19]. The height of the flanged hole wall for an initial hole diameter of 12mm was determined to be 7.56mm, as shown in Figure 5.

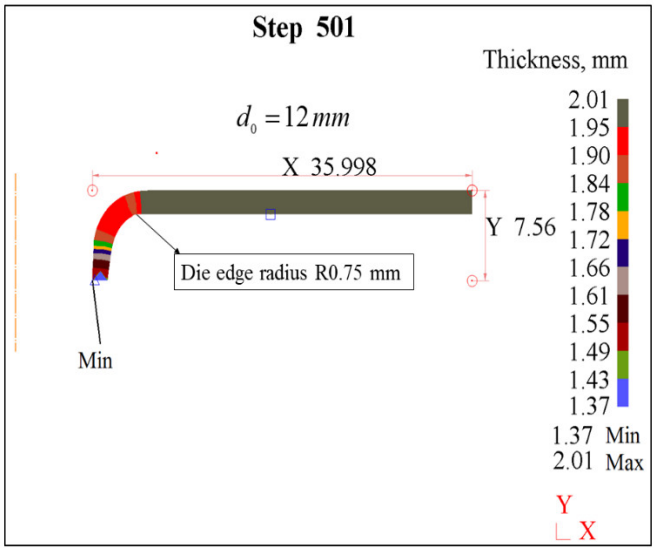

Figure 5. Height and Thickness Distribution of the Flanged Hole Wall

3.2. Experimental results

Figure 6 shows the specimens before and after the experiment. Direct observation of the appearance of damage is challenging, but closer examination under a ZEISS Axio Imager A2m microscope at 50x magnification revealed the onset of cracking in the flanged hole of the specimen with an initial diameter of d_0 = 12mm. Figure 7 displays the image of the edge of flanged hole wall for the blank with a diameter of d_0 = 12mm.

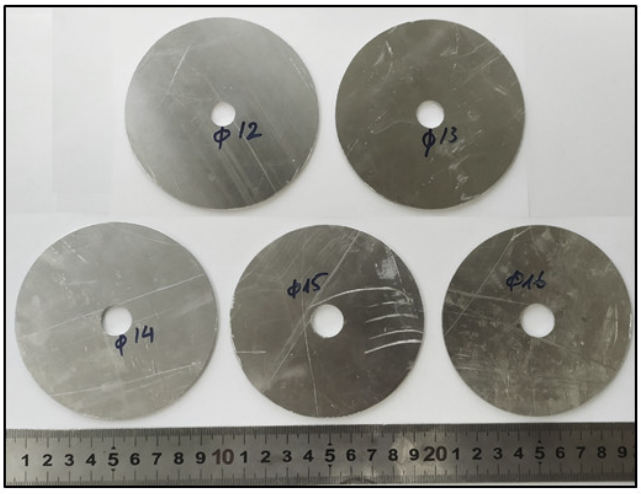

Workpieces

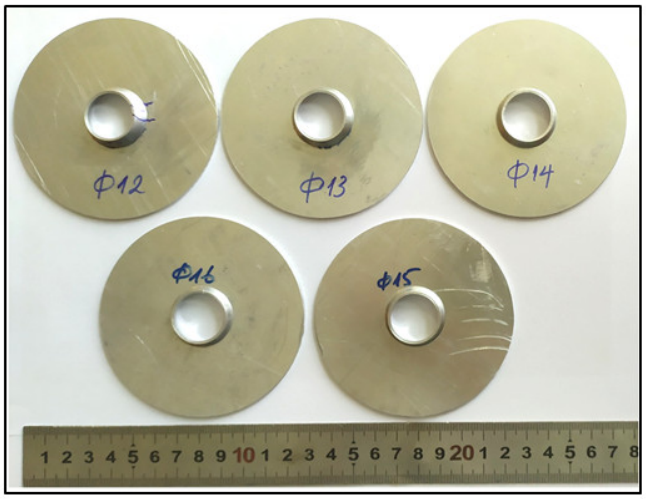

Figure 6. Blank Specimens and Hole-flanging Parts

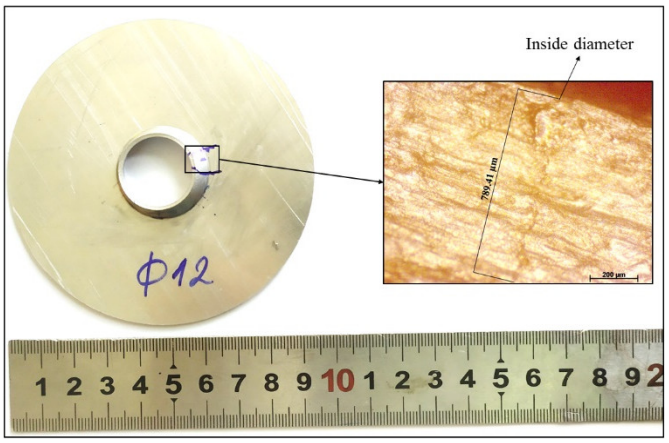

Figure 7. Hole-Flanging Part for the Blank with an Initial Diameter of 12mm

It can be observed that a very small crack, originating from the inner edge of the flanged hole wall (shown in Figure 3), is consistent with the simulation results. This crack has approximately 0.789mm in length and the thickness of the edge of the flanged hole wall is 1.35mm. This observation aligns with the maximum Cockroft-Latham damage value obtained from the simulation, 61.64MJ/m^3. The value only slightly exceeds the critical damage value of 61.49MJ/m^3. These findings demonstrated that the Cockroft-Latham ductile fracture criterion accurately predicted the occurrence of failure during the hole-flanging process, particularly at the location where the tangential tensile stress at the edge of the flanged hole wall is at its highest. This result is consistent with our previous study on the Erichsen cupping test and the combined deep drawing process [10]. The Cockroft-Latham ductile fracture criterion, therefore, proves to be a reliable predictor of failure during hole-flanging, even surpassing its predictive capability in the combined deep drawing process. Observation of the part obtained from the blank with an initial hole diameter of 13mm in Figure 8 revealed no cracks, aligning perfectly with the simulation results.

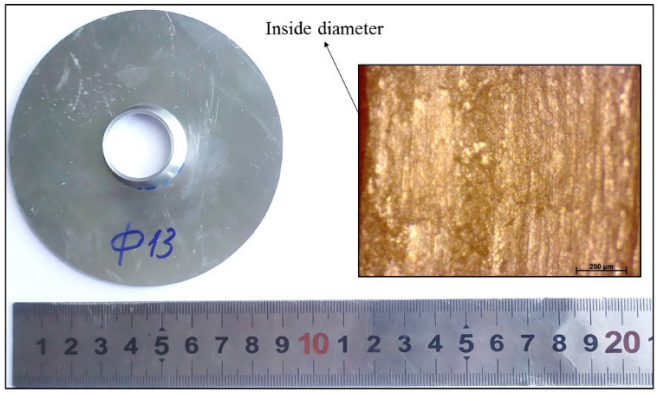

Figure 8. The edge of the flanged hole wall for the blank with an initial hole diameter of 13mm

The experimental results of the hole-flanging process for blanks with initial hole diameters d_0 corresponding to the simulations are presented in Table 1.

Table 1. Experimental and Simulation Results of the Hole-Flanging Process

d_0, mm	12	12.2	13	14	15	16
m_{HF}	0.6	0.61	0.65	0.7	0.75	0.8
Experiment	Failure	Limitting	Good	Good	Good	Good
Simulation	Failure		Good	Good	Good	Good

The height and minimum thickness of the flanged hole wall, as identified in both experiments and simulations, are presented in Figure 9. The numerical simulation results align closely with the experimental data. However, the simulations predicted a slightly lower height for the flanged hole wall and a greater minimum thickness compared to the experimental results. Despite these differences, the discrepancies between the simulations and experiments for both the height and the minimum thickness of the flanged hole wall are within 3%. It is observed that as the hole-flanging coefficient increases, the height of the flanged hole wall decreases, while the minimum thickness increases. Theoretical calculations for the thickness at the edge of the flanged hole wall can be determined using the formula [20]:

$$s_{min} = s_0\sqrt{m_{HF}} \quad (4)$$

Figure 9b shows that the theoretically calculated minimum thickness of the flanged hole wall is greater than that observed in both simulations and experiments.

This observation can be attributed to the theoretical calculations not accounting for material hardening, the bending of the material around the die edge, and the coefficient of friction between the blank and the tool.

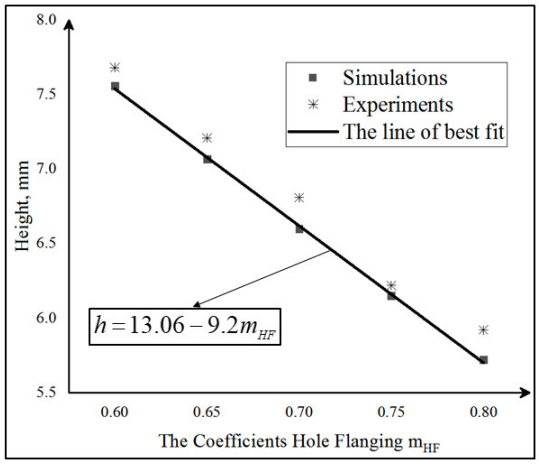

a)

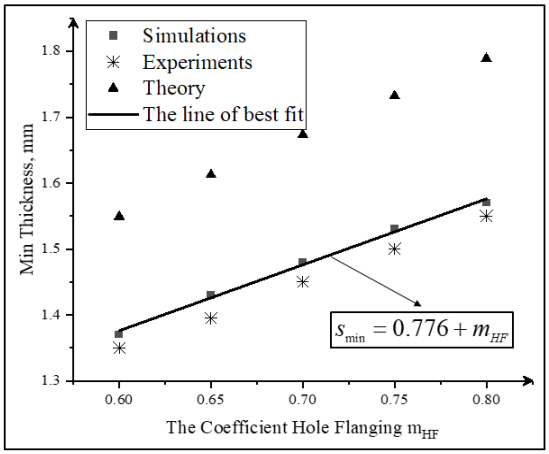

b)

Figure 9. Dependence of the minimum thickness (a) and the height (b) of the flanged hole wall on the hole-flanging coefficient

The approximate models for the height and minimum thickness of the flanged hole wall are given by the following equations:

$$h = 13.06 - 9.2m_{HF} \quad (5)$$

$$s_{min} = 0.776 + m_{HF} \quad (6)$$

The consistency between the simulation and experimental results supports the use of equations (5) and (6) for determining the height and minimum thickness of the flanged hole wall in cases of hole-flanging with wide clearance.

4. CONCLUSION

This study investigated the hole-flanging process with wide clearance, revealing that cracks initiated from the inner edge of the flanged hole wall where it contacts the punch. The hole-flanging ability of AA1050-O aluminum alloy sheet was characterized by a limiting hole-flanging coefficient of 0.61, as determined through both numerical simulations and experimental validation. The Cockroft-Latham ductile fracture criterion proved highly effective in predicting failure during the Hole-flanging process.

Equations were developed to relate the Cockroft-Latham damage value, minimum thickness, and height of the flanged hole wall to the hole-flanging coefficient. These equations provided valuable tools for engineers in designing hole-flanging operations for AA1050-O aluminum alloy sheets. In certain hole-flanging scenarios, the theoretical formula for determining the minimum thickness may yield inaccurate results, as it fails to account for critical factors such as material hardening, bending of the material around the die edge, and the coefficient of friction between the blank and the tool. For instance, materials that exhibit significant strain hardening, such as aluminum alloys and high-strength steels, undergo localized strengthening during cold deformation, which causes deviations from the theoretical formula. Moreover, small die edge radii exacerbate bending stresses, leading to additional thinning of the material that is not reflected in the theoretical model. Increased friction coefficients, often caused by inadequate lubrication or surface roughness, elevate tensile stress at the edge of the flanged hole, which further intensifies the thinning of the material. These limitations underscore the need to incorporate numerical simulations and experimental validation to address these complexities and improve the accuracy and relevance of thickness predictions in practical manufacturing processes.

ACKNOWLEDGMENT

This research was financially supported by the Le Quy Don Technical University under Project No. 23.1.08.

REFERENCES

[1]. V. Kumar, D. R. Kumar, "Influence of Hole Preparation Technique on Stretch Flangeability of Aluminium Alloys," *IOP Conf. Ser. Mater. Sci. Eng.*, 1307, 1, 012044, 2024. doi: 10.1088/1757-899x/1307/1/012044.

[2]. V. Kumar, D. Ravi Kumar, "Numerical and experimental investigation of hole flangeability of AA6061 alloy," *IOP Conf. Ser. Mater. Sci. Eng.*, 1284, 1, 012018, 2023. doi: 10.1088/1757-899x/1284/1/012018.

[3]. H. Yu, Q. Zheng, S. Wang, Y. Wang, "The deformation mechanism of circular Hole-flanging by magnetic pulse forming," *J. Mater. Process. Technol.*, 257, 2010, 54-64, 2018. doi: 10.1016/j.jmatprotec.2018.02.022.

[4]. F. Stachowicz, "Determination of the Hole-flangeability for thin Sheets," *Acta Mech. Slovaca*, 22, 4, 44-48, 2019. doi: 10.21496/ams.2018.033.

[5]. V. Paunoiu, G. Calvez, C. Maier, "Numerical and Experimental Investigation of Hole-flanging Process," *The Annals of "Dunarea de Jos" University of Galati, Fascicle V, Technologies in Machine Building*, 2016.

[6]. D. I. Hyun, S. M. Oak, S. S. Kang, Y. H. Moon, "Estimation of hole flangeability for high strength steel plates," *J. Mater. Process. Technol.*, 130-131, 9-13, 2002. doi: 10.1016/S0924-0136(02)00793-8.

[7]. M. Borrego, D. Morales-Palma, A. J. Martínez-Donaire, G. Centeno, C. Vallellano, "Analysis of formability in conventional Hole-flanging of AA7075-O sheets: punch edge radius effect and limitations of the FLC," *Int. J. Mater. Form.*, 13, 2, 303-316, 2020. doi: 10.1007/s12289-019-01487-2.

[8]. S. E. Seyyedi, H. Gorji, M. Bakhshi-Jooybari, M. J. Mirnia, "Comparison between conventional press-working and incremental forming in hole-flanging of AA6061-T6 sheets using a ductile fracture model," *Int. J. Solids Struct.*, 270, no. May, 112225, 2023. doi: https://doi.org/10.1016/j.ijsolstr.2023.112225 Get rights and content.

[9]. Y. Bai, T. Wierzbicki, "Application of extended Mohr-Coulomb criterion to ductile fracture," *Int. J. Fract.*, 161, 1, 1-20, 2010. doi: 10.1007/s10704-009-9422-8.

[10]. T. D. Hoan, T. T. Loan, T. Thi, V. Nga, H. Thi, M. Hue, "Combined Solution for Critical Damage Determination and Fracture Prediction in AA1050-O Alloy Sheets," *Metall. Mater. Trans. B*, 2024. doi: 10.1007/s11663-024-03124-z.

[11]. S. Bharti, A. Gupta, H. Krishnaswamy, S. K. Panigrahi, M. G. Lee, "Evaluation of uncoupled ductile damage models for fracture prediction in incremental sheet metal forming," *CIRP J. Manuf. Sci. Technol.*, 37, 499-517, 2022. doi: 10.1016/j.cirpj.2022.02.023.

[12]. V. K. Barnwal, S. Y. Lee, J. Choi, J. H. Kim, F. Barlat, "Performance review of various uncoupled fracture criteria for TRIP steel sheet," *Int. J. Mech. Sci.*, 195, no. September, 106269, 2021. doi: 10.1016/j.ijmecsci.2021.106269.

[13]. H. Talebi-Ghadikolaee, H. M. Naeini, M. J. Mirnia, M. A. Mirzai, H. Gorji, S. Alexandrov, "Ductile fracture prediction of AA6061-T6 in roll forming process," *Mech. Mater.*, 148, 103498, 2020. doi: 10.1016/j.mechmat.2020.103498.

[14]. Z. Pater, J. Tomczak, T. Bulzak, Ł. Wójcik, P. Walczuk, "Assessment of ductile fracture criteria with respect to their application in the modeling of cross wedge rolling," J. *Mater. Process. Technol.*, 278, no. November, 2020. doi: 10.1016/j.jmatprotec.2019.116501.

[15]. M. G. Cockcroft, D. J. Latham, "Ductility and the workability of metals," *Journal of the Institute of Metals,* 96, 1. 33–39, 1968.

[16]. J. W. Yoon, F. Barlat, J. J. Gracio, E. Rauch, "Anisotropic strain hardening behavior in simple shear for cube textured aluminum alloy sheets," *Int. J. Plast.*, 21, 12, 2426-2447, 2005. doi: 10.1016/j.ijplas.2005.03.014.

[17]. M. T. Mezher, O. S. Barrak, S. A. Nama, R. A. Shakir, "Predication of Forming Limit Diagram and Spring-back during SPIF process of AA1050 and DC04 Sheet Metals," *J. Mech. Eng. Res. Dev.*, 44, 1, 337-345, 2021.

[18]. D. K. Leu, T. C. Chen, Y. M. Huang, "Influence of punch shapes on the collar-drawing process of sheet steel," *J. Mater. Process. Technol.*, 88, 1, 134-146, 1999. doi: 10.1016/S0924-0136(98)00385-9.

[19]. T. C. Chen, "An analysis of forming limit in the elliptic hole-flanging process of sheet metal," *J. Mater. Process. Technol.,* 192-193, 373-380, 2007. doi: 10.1016/j.jmatprotec.2007.04.035.

[20]. M. V. Storozhev, E. A. Popov, *Theory of metal forming* (in Russian). Moscow: Mashinostroenie, 1977.

THÔNG TIN TÁC GIẢ

Trần Đức Hoàn[1], Tô Thanh Loan[2], Tạ Đức Cảnh[3]

[1]Khoa Cơ khí, Trường Đại học Kỹ thuật Lê Quý Đôn

[2]Trường Vật liệu, Đại học Bách khoa Hà Nội

[3]Công ty TNHH Cơ khí 83 (Nhà máy Z183)